GLOBAL MAPPING OF HEMATITE AT MARS USING VISIBLE OMEGA/MEx HYPERSPECTRAL DATA.
L. Riu[1], A. Ody[2], J. Carter[3,4], [1]European Space Astronomy Center (ESAC/ESA), [2]Independant researcher, [3]Laboratoire d'Astrophysique de Marseille (LAM), [4]Institut d'Astrophysique Spatiale. Contact: lucie.riu@esa.int

Introduction: Hematite has been detected at Mars both *in situ* and from orbit in different locations [1-5] but its occurrence frequency and distribution remain poorly known. The hematite deposits characterized from orbit by the TES instrument are thought to be products of liquid water alteration [1]. In parallel, hematite has also been detected *in situ* by the CheMin instrument on board the Curiosity rover, in the Vera Rubing Ridge in every sample analyzed [2, 3] and by the Microscopic Imager and Mini-TES on board Opportunity in Meridiani Planum [4]. Some of these detections were also confirmed by the CRISM instrument on board MRO [5]. These various detections could indicate subsequent episodes of warm and/or saline and/or acidic fluids alteration [2] and thus can be used to provide clues to the history of water at Mars.

Dataset: The OMEGA instrument (Observatoire pour la Minéralogie, l'Eau, les Glaces et l'Activité, [6]) on board Mars Express has been orbiting Mars for two decades providing numerous insights on the red planet overall mineralogy with more than 17000 hyperspectral images acquired covering the visible to infrared wavelength range. We use here the visible OMEGA data set that covers a range of wavelength from 0.58 µm to 0.97 µm enabling the detection of several potential hematite features. We selected a few tens of hyperspectral image cubes covering the region between 30° W and 20° E in longitude and -18° to +10° in latitude where the Sinus Meridiani and Aram Chaos hematite deposits are found [1] to be used as a benchmark for the detection of hematite using OMEGA data.

Methods: This study is a first step towards the global mapping of hematite using OMEGA hyperspectral images. We tested and selected several criteria based on CRISM spectral parameters [7] as well as new spectral parameters. The list of selected spectral parameters is indicated on Figure 1. Some forms of hematite can be detected by evaluating the band depth at 860 nm, although this feature can also be attributed to the presence of pyroxene providing false positive to the detection of hematite (see blue spectra in Figure 1, b). The shift in position between the two hematite deposits (Sinus Meridiani and Aram chaos in red and green respectively) could be due to a different mixture of hematite and/or other components.

To characterize the spectral behavior of the selected regions, we performed prior processing to the spectra. Firstly, we fitted the OMEGA spectra with a polynomial function (order 3) to estimate a continuum to be removed to the spectra (*e.g.* Figure 1, a). Then we applied the spectral parameter to the continuum-removed spectra. For some parameters ("Min", "Max" and R(0.73)/R(0.84)) this continuum-removed spectra is fitted a second time with a polynomial function (order 9) to smooth out the noise (solid line on Figure 1, b). We

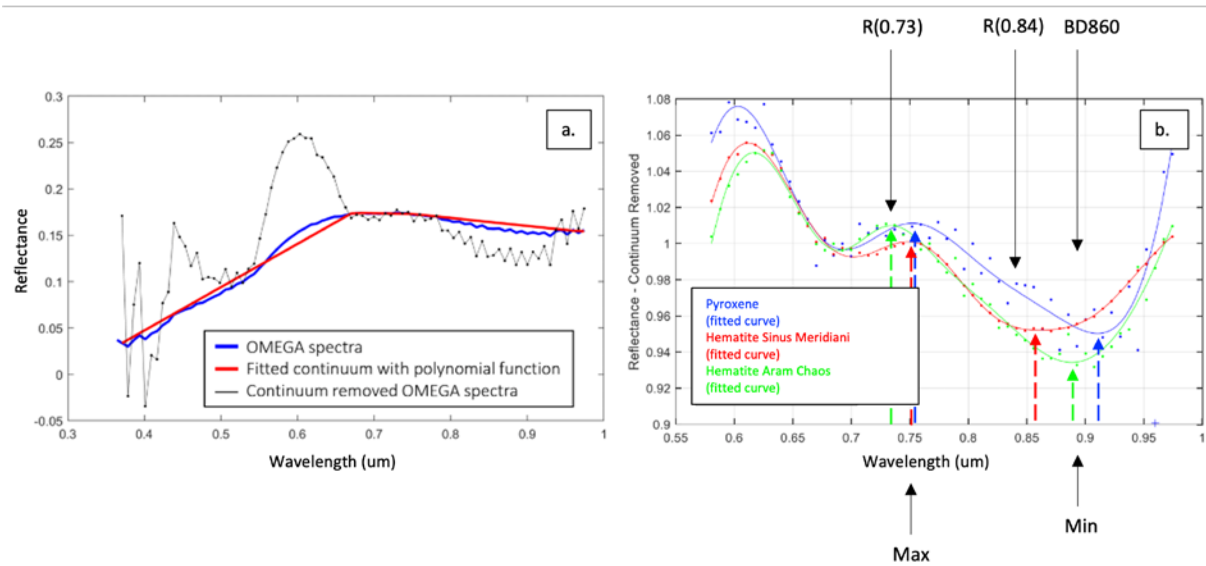

Figure 1 - (a) Characteristic OMEGA spectrum in blue, with a fitted continuum in red and the resulting continuum removed spectrum in black. (b) Continuum removed spectra of (a), fitted with a polynomial function of order 9. The different criteria tested: BD860, SH600, SH750, R(0.73)/R(0.84), are indicated on (b).

can see in the continuum removed spectra that the position and strength of the 860 nm feature (also referred to as "Min" on Figure 1, b) is changing depending on the region and *a priori* mineralogy: pyroxene (shown in blue on Figure 1) or hematite (shown in red and green on Figure 1). Additionally, we observed that the maxima (referred to as "Max" on Figure 1, b) at 750 nm and the minimum of reflectance ("Min" in Figure 1) in this spectral region also vary in position and might be used to discriminate between pyroxene and hematite and be used for the mapping of the latter.

The slope between "Max" and "Min" also seems to be stronger for hematite than for pyroxene and is computed as the ratio between the reflectance at 730 nm and 840 nm. The maps (Figure 2) shows the detection at the pixel scale based on selected criteria that show potential in discriminating hematite and pyroxene: BD860, R(0.73)/R(0.84) and an evaluation of the "Max" and "Min" positions (see Figure 1, b). Other spectral indexes were tested but did not result into convincing detection maps.

We can see that the combination of the spectral indexes (Figure 2, d) improves the quality of the detection by highlighting high hematite abundance areas, in agreement with TES detections, and removing some false positive (either due to pyroxene detection or artifacts, as indicated on Figure 2, a). A "new positive" or "false positive" area is detected in the Northern East of Sinus Meridiani and will need to be investigated further.

Future steps: We were able to test several spectral criteria and combination of criteria to characterize already well-known hematite deposits in Sinus Meridiani and Aram Chaos. This first analysis step shows that hematite can be uniquely detected and mapped with OMEGA. Although these criteria and combination of criteria must be tested and evaluated over a wider area to minimize the detections of false positive and unsure the detection of all hematite deposits, these first preliminary local maps show the potential to provide a high spatial resolution (< 1km/px) global map of this mineral using a combination of spectral criteria on OMEGA spectra. This global mapping effort will be conducted in the future months, hoping to provide new insights onto the Martian aqueous alteration history.

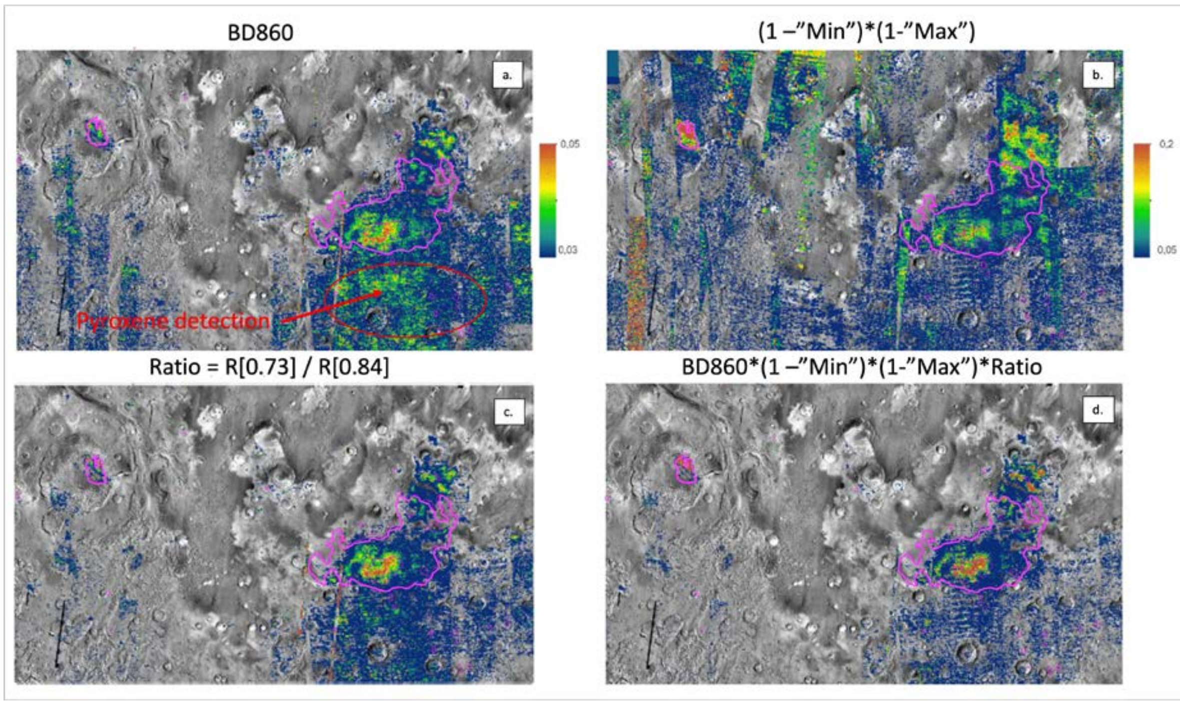

Figure 2 - Detections maps of hematite based on different spectral indexes. (a) Band depth at 860 nm. (b) (1-"Min")*(1-"Max"). (c) Ratio of reflectance at 730 nm and 840 nm. (d) A combination of the three criteria. The pink contour represents the contour of major hematite detections by TES [1].

References: [1] Christensen et al., 2001, JGR, vol. 106, E10, pages 23873 – 23885. [2] Rampe et al., 2020, JGR – Planets, 125, e2019JE006306. [3] Fraeman et al., 2020, JGR – Planets, 125, e2020JE006527. [4] Calvin et al, 2008, JGR – Planets, 113, E12S37, doi:10.1029/2007JE003048 [5] Fraeman et al., 2013, Geology, 41(10), 1103–1106, doi:10.1130/G34613.1. [6] Bibring et al., 2004, Mars Express: the scientific payload, 2004ESASP1240…37B. [7] Viviano-Beck et al., 2014, JGR – Planets, 119, 1403-1437, doi:10.1002/2014JE004627.